The Egyptian Journal of Remote Sensing and Space Sciences xxx (xxxx) xxx

HOSTED BY

Contents lists available at ScienceDirect

The Egyptian Journal of Remote Sensing and Space Sciences

journal homepage: www.sciencedirect.com

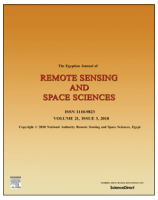

Research Paper

Landslide susceptibility assessment using Frequency Ratio, a case study of northern Pakistan

Hawas Khan [a], Muhammad Shafique [b,*], Muhammad A. Khan [a], Mian A. Bacha [b], Safeer U. Shah [b], Chiara Calligaris [c]

[a] Karakorum International University, Gilgit, Pakistan
[b] National Centre of Excellence in Geology, University of Peshawar, Peshawar, Pakistan
[c] University of Trieste, Department of Mathematics and Geosciences, Via Weiss 2, Trieste 34128, Italy

ARTICLE INFO

Article history:
Received 13 November 2016
Revised 2 February 2018
Accepted 19 March 2018
Available online xxxx

Keywords:
Landslides
Frequency ratio
Remote sensing
Susceptibility mapping
Northern Pakistan

ABSTRACT

The northern Pakistan is attributed with rough terrain, active seismicity, monsoon rains, and therefore hosts to variety of geohazards. Among the geohazards, landslides are the most frequent hazard with devastating impacts on economy and society. However, for most of the northern Pakistan, landslide susceptibility maps are not available which can be used for landslide hazard mitigation. This study aims to develop a remote sensing based landslide inventory, analysing their spatial distribution and develop the landslide susceptibility map. The area, selected for this study is comprised of Haramosh valley, Bagrote valley and some parts of Nagar valley, in the Central Karakoram National Park (CKNP) in Gilgit-Baltistan, northern Pakistan. The SPOT-5 satellite image was used to develop a landslide inventory which was subsequently verified in the field. The landslide causative factors of topographic attributes (slope and aspect), geology, landcover, distances from fault, road and streams were used to evaluate their influence on the spatial distribution of landslides. The study revealed that the distance to road, slope gradient has the significant influence on the spatial distribution of the landslides, followed by the geology. The derived results were used in the Frequency ratio technique to develop a landslide susceptibility map. The developed landslide susceptibility map can be utilized for landslide mitigation in the study area.

1. Introduction

Landslide is a complex geohazard, with devastating impacts on sustainable socio-economic development, in mountainous terrains. Northern Pakistan is one of the most landslide prone regions, which can be attributed to the rugged topography, active seismicity, monsoon rains and anthropogenic activities on unstable slopes (Hewitt, 1998, Derbyshire et al., 2001, Kamp et al., 2008, Shafique et al., 2016). The province of Gilgit-Baltistan, in northern Pakistan, is frequently and severely affected by landslides in the past, and prone to more landslides induced devastations in the future. In the recent past, the Attabad rockslide on 4th January 2010 in the region have killed 19 people, displaced 6000 people, blocked the river Hunza for five months that leads to about 14 km natural lake which still exists, and submerging 19 km of the strategic Karakorum Highway (KKH). Despite the threatening landslides in the region, the landslide susceptibility maps are not available for the most of the area, which can be used for landslide hazard assessment and mitigation.

Satellite images and aerial photos with extensive spatial and repetitive coverage, are effectively used in Geographic Information System (GIS) for landslide detection, monitoring and susceptibility assessment (Weissel and Stark, 2001, Chen et al., 2016, Shafique et al., 2016, Wang and Li, 2017)). Landslide inventory is often developed from satellite images, however; the utilized images shall comply with the criteria proposed by Harp et al. (2011). Satellite images such as the Landsat, ASTER and Sentinel are available free of costs with global coverage and therefore can be effectively utilized to develop landslide inventory on a regional scale. Fine resolution images such as the IKONOS, QuickBird, SPOT and WorldView are effectively utilized for developing landslide inventory at a local scale, however, their high price, narrow swath width and long revisit time, limit their application for regional scale studies

Peer review under responsibility of National Authority for Remote Sensing and Space Sciences.
* Corresponding author.
E-mail address: shafique@uop.edu.pk (M. Shafique).

https://doi.org/10.1016/j.ejrs.2018.03.004
1110-9823/

(Shafique et al., 2016). Visual and digital image classification techniques are effectively used to demarcate landslides from satellite images that should be subsequently verified in the field. Spatial distribution and intensity of landslides are mainly controlled by the causative factors, including lithology, tectonics, geomorphology, topography, precipitation and anthropogenic factors (Kamp et al., 2008, Shafique et al., 2016). These causative factors are often effectively computed from the satellite images and Digital Elevation Model (DEM). The landslide inventory is usually compared with the landslide causative factors, to determine their influence on the spatial distribution and intensity of landslides, and eventually; develop a landslide susceptibility map.

Techniques for landslide susceptibility assessment can be divided in quantitative and qualitative (Yalcin et al., 2011, Wang and Li, 2017). Quantitative techniques mainly rely on evaluating the probability of sliding, by analysing the relationship between causative factors and landslide inventory (Erener et al., 2016). Quantitative techniques for landslide susceptibility assessment, include logistic regression model (Nefeslioglu et al., 2008, Chauhan et al., 2010) weight of evidence model (Dahal et al., 2008, Ilia and Tsangaratos, 2016) frequency ratio (Reis et al., 2012, Umar et al., 2014, Wu et al., 2016) index of entropy model (Devkota et al., 2013), fuzzy logic (Rostami et al., 2016) and support vector machine (Tien Bui et al., 2016). Qualitative techniques are subjective, and traditionally use the landslide inventory to demarcate the sites of similar topographical, geological and geomorphological characteristics that are susceptible to sliding (Yalcin, 2008). Some of the qualitative techniques such as analytic hierarchy process (AHP), however, also consider the ranking and weighting concept, and may be called semi-quantitative in nature (Yalcin, 2008, Hung et al., 2015). AHP is based on the heuristic approaches, which mainly consider expert opinion about an area (Saaty, 1980, Yalcin, 2008, Reis et al., 2012, Kayastha et al., 2013, Mansouri and Reza, 2014). These techniques for landslide susceptibility assessment at a regional scale are applied, using spatial data often derived from remote sensing and secondary sources; and analysed in GIS.

Demarcating the areas, with high potential for landslides through susceptibility assessment, can be used by the decision makers for formulating and implementing the landslide mitigation strategies. However, for the landslide prone northern Pakistan, the landslide susceptibility maps are rarely available. Therefore, aim of this study is to develop a remote sensing derived landslide inventory, analyse their spatial distribution by comparing with causative factors, and a develop landslide susceptibility map using frequency ratio method.

2. Study area

The study area is situated in the Central Karakoram National Park (CKNP) and comprised of Haramosh valley, Bagrote valley and parts of Nagar valley in the Gilgit-Baltistan, Pakistan (Fig. 1). The Central Karakoram National Park (CKNP) is one of the largest (10000 km^2) protected regions in Gilgit-Baltistan with considerable natural resources. It consists of large alpine glaciers and fresh water, fed by high mountains glaciers.

Elevation of the area ranges from 1400−7788 m above sea level and slopes ranging from 50−70°. The area is most prone frequent landslides, given the rugged topography, active seismicity, fractured geology, climatic factors and anthropogenic activities on unstable slopes (Fig. 2). The maximum temperature in summer exceeds 40 °C, despite the fact that mean monthly winter temperature fall below 0 °C in the main valleys above 2300 m asl. In 2001, a huge rock avalanche hit Barchi Haramosh-Gilgit and buried a small settlement known as "Goon".

The study area is located in one of the most seismically active regions on earth, with active Himalayan ranges in north, Hindu Kush mountain ranges in northwest and Suleiman mountain ranges in southwest. High seismic hazard in Pakistan and adjacent Indian and Afghanistan regions is due to northward movement of the Indian tectonic plate at a rate of 31 mm/year (Bettinelli et al., 2006) which is subducting beneath the Eurasian continent. This collision of the Indian and Eurasian plates resulted in the development of world highest mountain ranges i.e. Karakoram, Himalaya and Hindu Kush mountain ranges (Sayab and Khan 2010). The combined impact of active tectonics, high seismicity, rough topography, fractured geology, weather and anthropogenic activities on the unstable slopes leads to frequent and devastating landslides in the study area (Fig. 3).

3. Material and methods

3.1. Remote sensing data

The Advanced Spaceborne Thermal Emission and Reflection Radiometer (ASTER) derived Digital Elevation Model (DEM) with spatial resolution of 30 m, was used to compute terrain slope and aspect for the study area. Landslide inventory and landcover maps were developed from the SPOT-5 imagery (spatial resolution of 2.5 m and acquisition date of 20-September-2013).

3.2. Landslide inventory

Landslide inventory of the study area was developed from the SPOT-5 imagery using visual image classification technique. The mapped landslides, were subsequently verified in the field and the outlines of the landslides were modified accordingly.

3.3. Landslide causative factors

Spatial distribution and intensity of the landslides are significantly controlled by the surrounding topography, geology, tectonic features, weather conditions, landcover and anthropogenic factors. Therefore, evaluating the impact of these causative factors on spatial distribution of the landslides is of significant importance to understand their operating mechanism, and subsequently develop a landslide susceptibility map.

3.3.1. Terrain slope

Terrain slope mainly determine the spatial distribution and intensity of landslides (Shafique et al., 2016). Terrain slope of the study area was computed from the ASTER DEM using the ArcGIS 10.2. It was calculated using a 3×3 moving window based on the algorithm of Burrough and McDonell (1998). The derived slope map was subsequently classified in eight classes including <10, 10–20, 20–30, 30–40, 40–50, 50–60, 60–70 and >80 (Fig. 6a).

3.3.2. Terrain aspect

Terrain aspect is the slope direction, and because of its significant impact on the vegetation cover, moisture retention and soil strength; it can influence landslide initiation (García-Rodríguez et al., 2008, Basharat et al., 2014). Terrain aspect of the study area was computed from the ASTER DEM, using a 3×3 moving window in the ArcGIS 10.2 (Burrough and McDonell, 1998) (Fig. 6b).

3.3.3. Lithology

It is widely accepted that lithological characteristics strongly effect the physical properties, such as strength and permeability of the surface and sub-surface material; and therefore affect the likelihood of land sliding (Kamp et al., 2008). The lithology

Please cite this article as: H. Khan, M. Shafique, M. A. Khan et al., Landslide susceptibility assessment using Frequency Ratio, a case study of northern Pakistan, The Egyptian Journal of Remote Sensing and Space Sciences, https://doi.org/10.1016/j.ejrs.2018.03.004

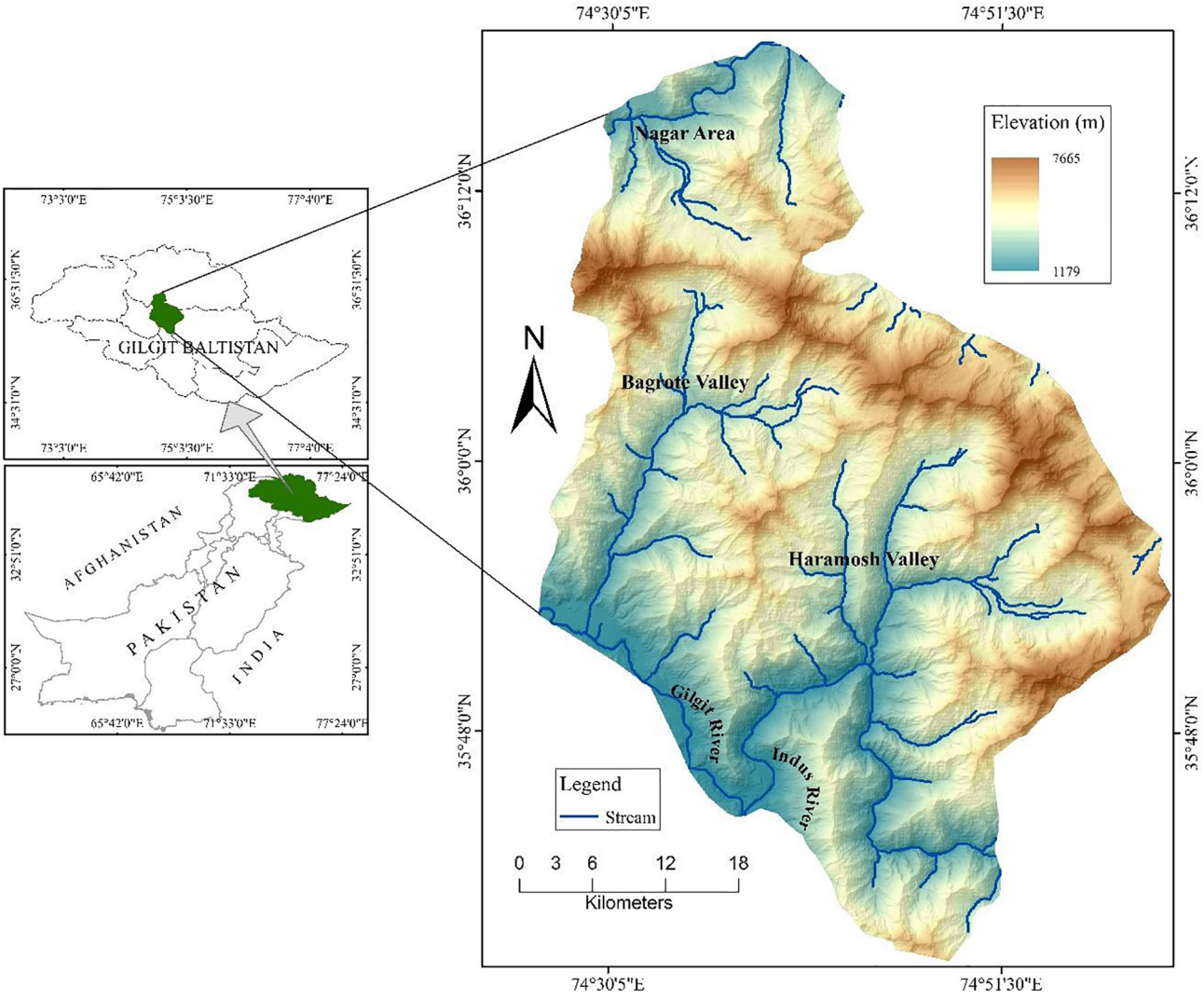

Fig. 1. Location map of the study area.

together with terrain slope determine the nature and intensity of landslide (Chen et al., 2012, Faraji Sabokbar et al., 2014). Geological map of the study is shown in Fig. 6c after Searle and Khan (1996) (Fig. 6c).

Geology of the Haramosh valley can be discussed in the context of the geology of Nanga Parbat Haramosh massif as described by Misch (1949), Wadia (1961), Butler and Prior (1988), Madin et al. (1989) and Treloar amd Coward (1991). It consists of an ancient Orthogneiss complex (the Nanga Parbat Gneiss of Misch, 1949) which has been divided into the Shengus and Iskere gneisses by Madin and Lawrence (1989). These Proterozoic age gneisses have been extensively deformed before Himalayan tectonics. The Kohistan sequence is mainly composed of various types of meta basics such as the Shuta Gabbro (Madin and Lawrence, 1989) together with volcanic rocks and sediments present in the northern edge (Pudsey et al., 2011). Near the confluence of the Indus and Gilgit rivers, the metabasic rocks are cross-cut by a cluster of biotite granite sheets and lamprophyres (Petterson and Windley, 1985) which are deformed into the Main Mantle Thrust in the Indus Gorge. In the Indus Gorge near Sassi, the Main Mantle Thrust is characterized by large interleaved units derived from the Kohistan and Indian continent sequence which have large discontinuities in their structures and are highly susceptible for landslide.

Geology of the Bagrote Valley, consists of Chalt Group (Searle and Khan, 1996) and is characterized by heterogeneous volcanic and sedimentary rocks, exposed across the valley. In the southern parts of the valley, the contact between the Kohistan arc sequence and Chalt Group is exposed at the Datuchi village. The large number of diorites and granites, which belong to younger igneous phases, intruded into the Chalt group. The association of *meta*-sediments with tuffs and basaltic to andesitic lavas crop out in some places of Bagrote Valley. The ultramafic rocks of the Bagrote valley are part of the Dobani-Dasau ultramafic lineament strip. The Chalt group and ultramafic sequence considered as diverse nature are more prone to landslides. In parts of the Nagar valley, the weathering characteristic of Terigeneous Formation, conglomerate and amphibolites have various structure discontinuities and are prone to landslide. Quaternary deposits are exposed in the whole study area and is highly susceptible for land sliding.

3.3.4. Land cover

Land cover has a strong influence on the distribution of landslides, often, forested area have fewer landslides compare to the barren areas. Vegetated land cover with strong root system, provide the mechanical and hydrological effects that often stabilize the slopes (García-Rodríguez et al., 2008). Land cover of the study area was digitized from the acquired SPOT-5 image and

Please cite this article as: H. Khan, M. Shafique, M. A. Khan et al., Landslide susceptibility assessment using Frequency Ratio, a case study of northern Pakistan, The Egyptian Journal of Remote Sensing and Space Sciences, https://doi.org/10.1016/j.ejrs.2018.03.004

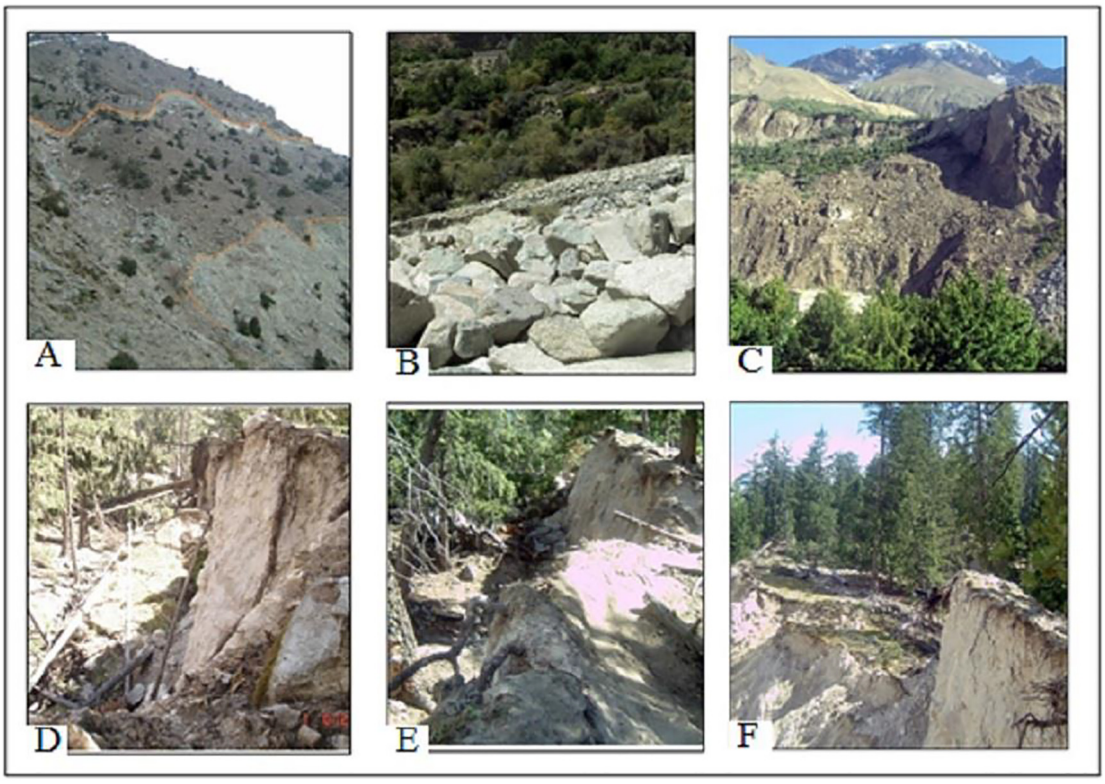

Fig. 2. Active landslides in the study area, a). Active landslide in Khaltaro Haramosh the orange color line on the photograph (top and lower part) indicates scrap and toe of landslide, b). Debris flow in Bagrote valley, c). Active rock fall in Phakar village Nagar valley, d, e and f). Rotational landslides in Godaye area-Haramosh valley Gilgit.

subsequently verified in the field (Fig. 6d). The landcover of the area was classified in water body, forest and shrub land, barren land, alpine pasture, spare grass, irrigated agricultural land, permanent snow and glacier.

3.3.5. Fault lines

Spatial distribution and nature of fault lines mainly determine the distribution and intensity of co-seismic landslides (Kamp et al., 2008, Lin and Guo, 2008, Peduzzi, 2010). Fault lines of the area, was extracted from the geological map of the area, after Searle and Khan (1996). Distance to the fault was divided into six buffer zones at 50 m intervals, using ArcGIS 10.2. Software (Fig. 6e).

3.3.6. Road network

In mountainous terrain, the construction of communication network including roads and railway, often leads to the destabilization of slope and eventually landsliding (Shafique et al., 2016). To evaluate the impact of road network on the landslides in the study area, the road network was extracted from the acquired SPOT-5 images and was subsequently verified in the field. Subsequently, distance from the road was computed from the road at the interval 100 m using ArcGIS software (Fig. 6f).

3.3.7. Streams network

Streams can play an adverse role in the stability of a slope, by undercutting due to toe erosion and by saturating the slide toe, due to increase in water infiltration (Gorum et al., 2011). To evaluate the impact of the streams, on distribution of the landslides, the stream network for the study area was computed from the ASTER DEM using ArcHydro tools (ESRI, 2017). The streams with accumulation area of more than 20 Km^2 were extracted. The distance from the streams was divided into six buffer zones with interval of 20 m in ArcGIS software (Fig. 6g).

These developed landslide causative factors were compared with the landslide inventory to evaluate their influence on spatial distribution of landslides and develop a landslide susceptibility map.

3.4. Landslide susceptibility mapping

For landslide susceptibility mapping, it is important to assume that the spatial distribution of landslides are influenced by the landslide causative factors, and that future landslides will occur under the same conditions as the past landslides (Lee and Talib, 2005). In this study, we have used Frequency Ratio (FR) for landslide susceptibility mapping.

3.4.1. Frequency ratio

Understanding the area specific, physical conditions and processes for triggering the landslides is of significant importance to evaluate the probability of landslides. Frequency ratio is a quantitative technique for landslide susceptibility assessment using GIS techniques and spatial data (Bonham-Carter, 1994, Lee and Talib, 2005, Chen et al., 2016, Chen et al., 2016, Ding et al., 2017). The frequency ratio (FR) technique is frequently and effectively used for landslide susceptibility mapping (Yilmaz, 2009, Reis et al., 2012, Umar et al., 2014, Chen et al., 2016, Wu et al., 2016, Wang and Li, 2017). It is based on the quantified association between the landslide inventory and the landslide causative factors (Reis et al., 2012). To obtain the frequency ratio (FR) for each class of the causative factors, a combination has been established between the landslide inventory map and factor map using the Eq. (1) (Mondal and Maiti, 2013).

$$Fr = \frac{\boldsymbol{Npix}(1)/\boldsymbol{Npix}(2)}{\sum \boldsymbol{Npix}(3)/\sum \boldsymbol{Npix}(4)} \quad (1)$$

Please cite this article as: H. Khan, M. Shafique, M. A. Khan et al., Landslide susceptibility assessment using Frequency Ratio, a case study of northern Pakistan, The Egyptian Journal of Remote Sensing and Space Sciences, https://doi.org/10.1016/j.ejrs.2018.03.004

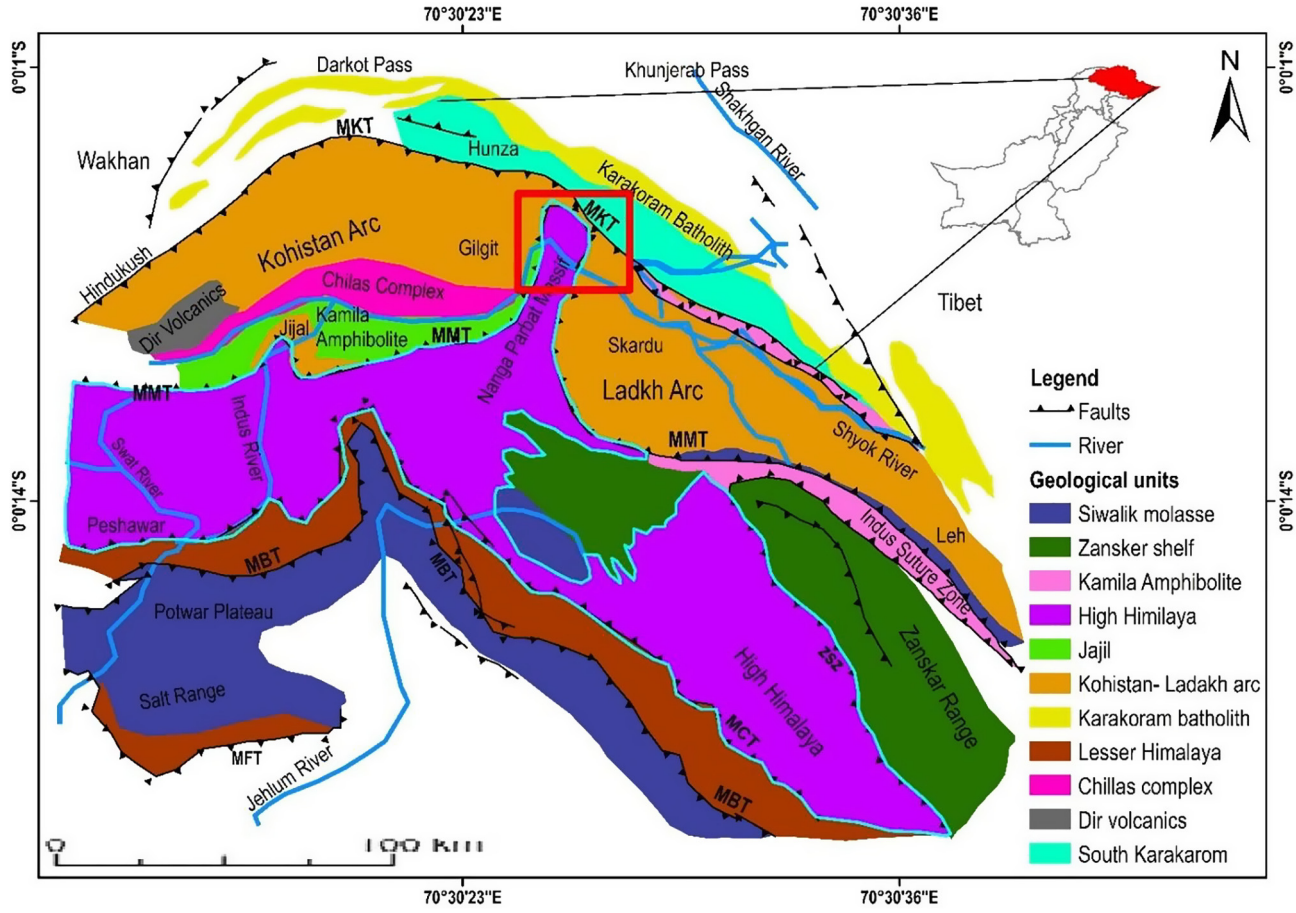

Fig. 3. Regional tectonic setting of the Shyok/Northern Suture Zone between the Asian continental margin (Karakoram Mountain) and the Kohistan-Ladkh Arc and the Nanga Parbat Haramosh Massif. The red square demarcates the study area.

N pix (1) = The number of pixels containing landslide in a class
N pix (2) = Total number of pixels of each class in the whole area
$\sum$ *N pix* (3) = Total number of pixels containing landslide
$\sum$ *N pix* (4) = Total number of pixels in the study area

The derived frequency ratio is summed to develop a Landslide Susceptibility Index (LSI) map using Eq. (2) (Lee and Talib, 2005)

$$LSI = Fr_1 + Fr_2 + Fr_3 + Fr_4 + \ldots\ldots\ldots + Fr_n \quad (2)$$

where Fr is the frequency ratio, and n is the number of selected causative factors.

According to the technique, the ratio is that of the area where the landslides is occurred, to the total area, so that the value of 1 is an average value. If the value is greater than 1, it means the percentage of the landslide is higher than the area and indicate a higher correlation, whereas values lower than 1 indicate a lower correlation (Akgun et al., 2007). The LSI map is reclassified to develop a landslide susceptibility map. The methodology adopted for the study is shown in Fig. 4.

4. Results and discussion

4.1. Landslide inventory

Based on the SPOT-5 images and field visit, 314 landslides were mapped with a total area of 112.53 Km^2 (Fig. 5). Majority of the landslides are complex landslide (Fig. 2d and f). Rock slides in the area are mainly because of the rock discontinuities along joints, fractures, bedding plane and steep terrain gradient. Debris flow are mainly triggered by the heavy rainfall and snow melt. Rotational landslides are mainly associated with the toe erosion and undercutting of the recent terraces.

4.2. Landslide causative factors

The causative factors used in the study are given in the Fig. 6. The assigned weights to each class of the causative factors is given in the Table 1. The derived weights shows that the terrain slope map (Fig. 6a) has a significant impact on the landslide distribution, which is in agreement with other mountainous areas (Shahabi et al., 2014). Occurrences of landslides increases with increase in terrain gradient, however, weight is reduced for terrain slope of >70°. The lower landslide frequency at the slope angle of >70° (Fig. 7a), is due to the presence of cliff without colluvium cover. The terrain with slope of 50–60° is most prone for the landslides with frequency ratio of 1.23 and the terrain with slope gradient of <10° is least prone to landslides with frequency ratio of 0.37 (Table 1).

The frequency ratio for the aspect map shows that the southeast, east and west facing aspect has highest frequency ratio values (Table 1). Southeast aspect got the maximum weight of 1.38 followed by east with 1.37 (Table 1). The lithological units in the geological map (Fig. 6c) have significantly influence on the spatial distribution of landslides. Table 1 shows that, among the geological units, the Terigenous formation and Quaternary deposit as the lose material, are most prone for landslides with frequency ratio of 1.89 and 1.73, respectively (Table 1). The area is range of 40–100 m from the streams are observed as hosting most of the mapped

Please cite this article as: H. Khan, M. Shafique, M. A. Khan et al., Landslide susceptibility assessment using Frequency Ratio, a case study of northern Pakistan, The Egyptian Journal of Remote Sensing and Space Sciences, https://doi.org/10.1016/j.ejrs.2018.03.004

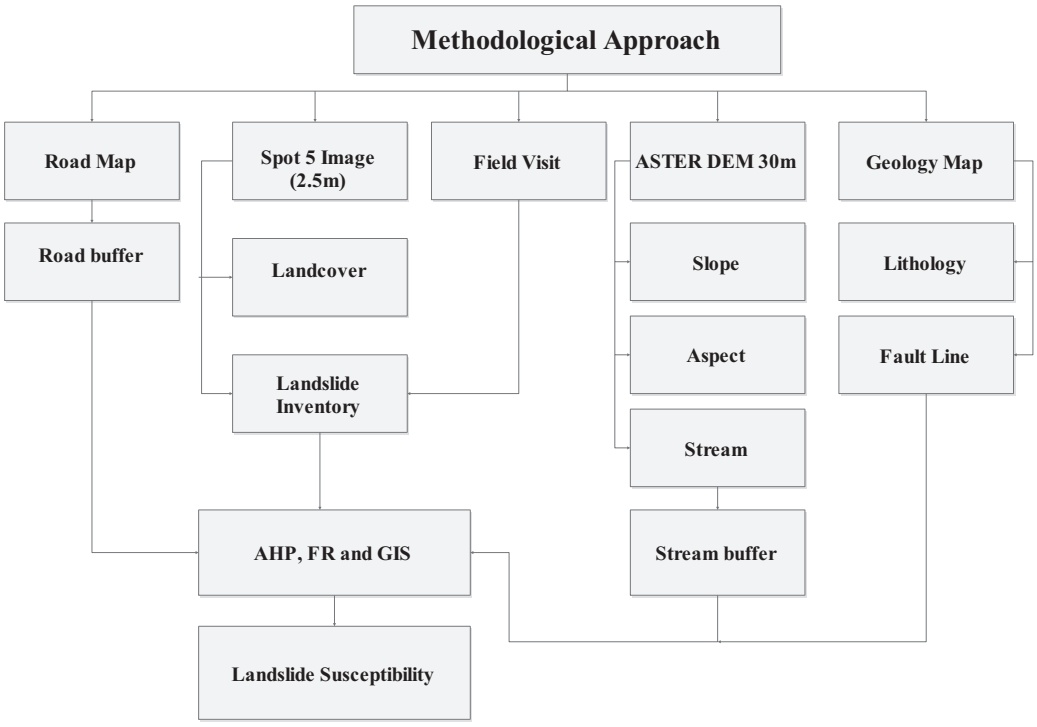

Fig. 4. Flowchart of the methodology adopted for the study.

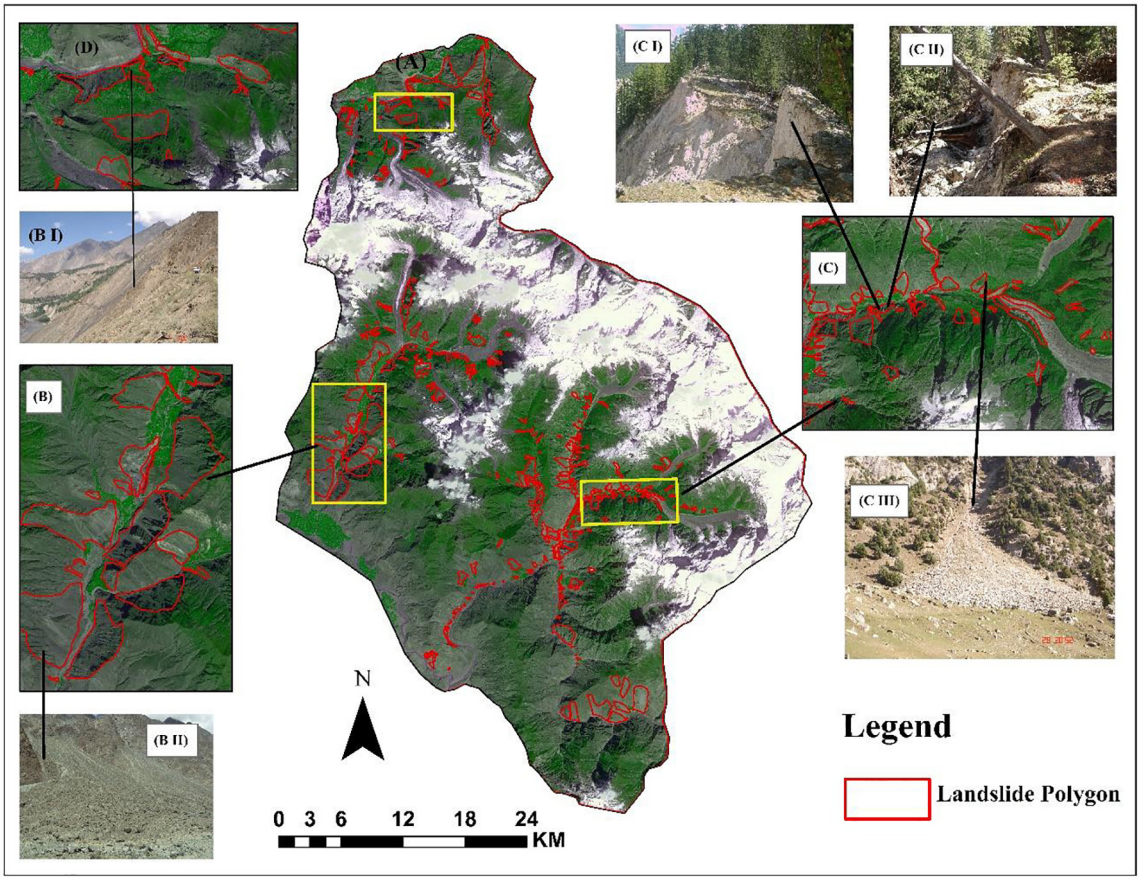

Fig. 5. (a) Landslide inventory in the study area, (b) and (c) magnified portions from the study area, BI and BII are active debris flow in Bagrote Valley, pictures taken during the field visit in June 2016. CI and CII are rotational landslides in Kutwall area Haramosh valley, pictures and CIII is a complex landslide picture taken in the field in June 2016.

Please cite this article as: H. Khan, M. Shafique, M. A. Khan et al., Landslide susceptibility assessment using Frequency Ratio, a case study of northern Pakistan, The Egyptian Journal of Remote Sensing and Space Sciences, https://doi.org/10.1016/j.ejrs.2018.03.004

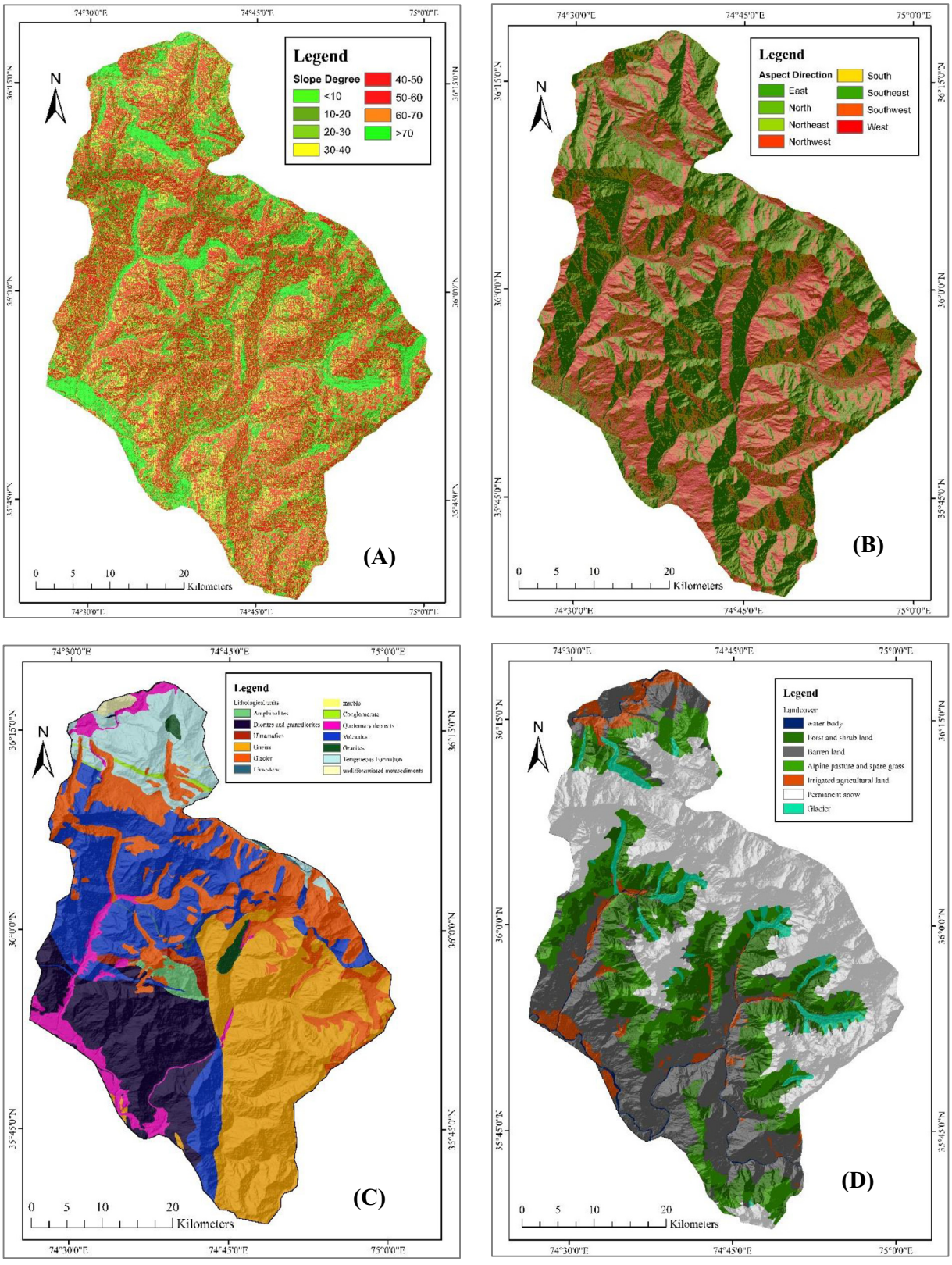

Fig. 6. Landslide causative factors used in the study (a) slope, (b) aspect, (c) geology, (d) landcover map, (e) distance to fault, (f) distance to road and (g) distance to stream.

landslides (Table 1). The mapped fault lines have significant influence on the spatial distribution of the landslides. The area in the vicinity of the mapped fault lines shows high frequency ratio (Table 1). In the study area, the road network has the highest influence on the spatial distribution of landslides with highest frequency ratio (Derbyshire et al., 2001). The area in the vicinity of 100 m buffer, of the roads, has the highest frequency ratio of 3.85, followed by 3.75 for the buffer of 101–200 m (Table 1). This can be attributed to the fact the uncontrolled blasting and excavation during the road construction on these fragile slopes leads to

Please cite this article as: H. Khan, M. Shafique, M. A. Khan et al., Landslide susceptibility assessment using Frequency Ratio, a case study of northern Pakistan, The Egyptian Journal of Remote Sensing and Space Sciences, https://doi.org/10.1016/j.ejrs.2018.03.004

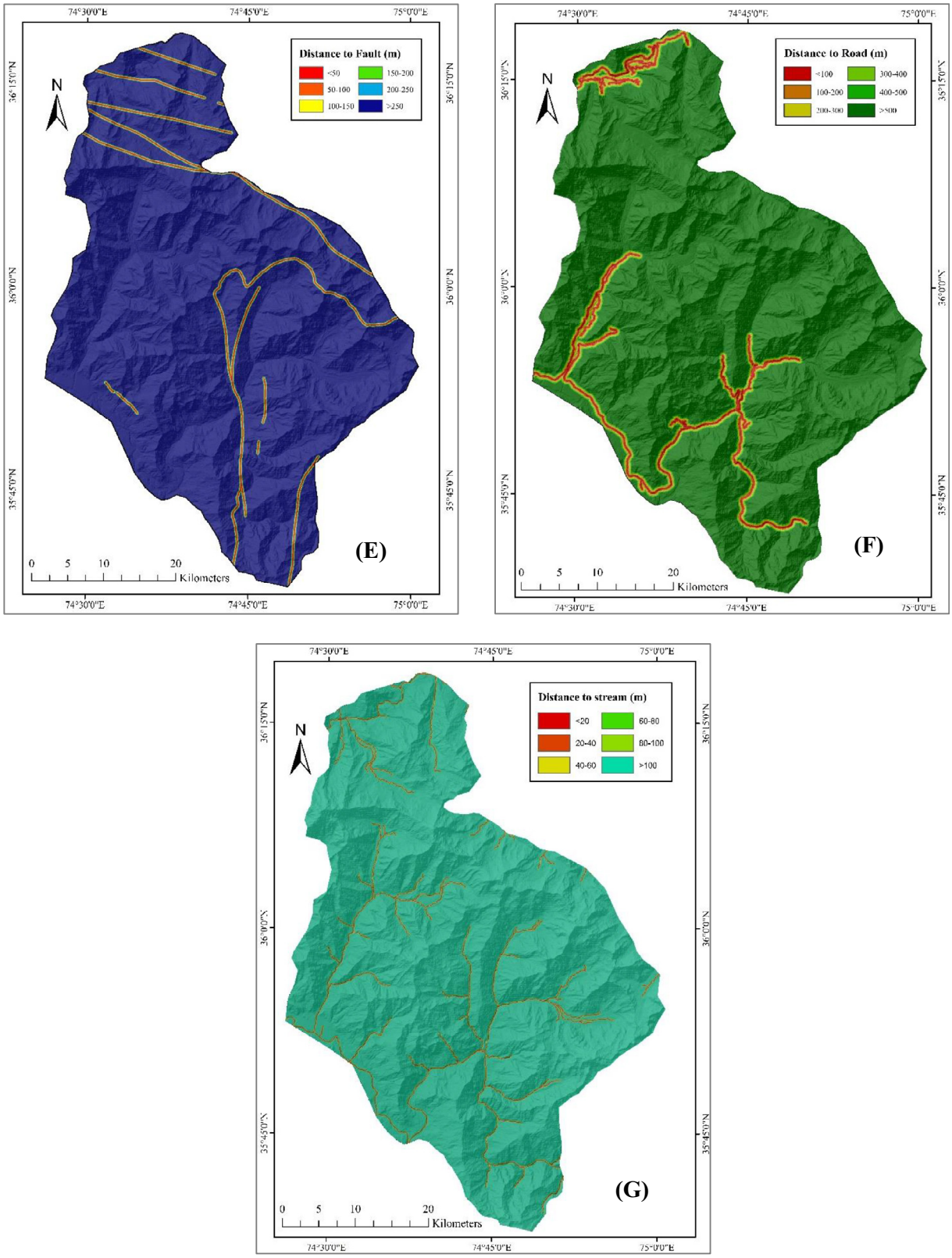

Fig. 6 (*continued*)

frequent land sliding (Devkota et al., 2013). Among the land covers, the barren land and irrigated agriculture land have the highest frequency ratio with 2.82 and 1.22 respectively (Table 1). As expected, the minimum frequency ratio values were noticed for the forest, shrub land and alpine pasture.

4.3. Landslide susceptibility index map

The derived frequency ratio for the selected causative factors classes, were combined in GIS to develop a LSI map (Fig. 8). The LSI map is reclassified in four classes i.e. low, moderate, high and

Please cite this article as: H. Khan, M. Shafique, M. A. Khan et al., Landslide susceptibility assessment using Frequency Ratio, a case study of northern Pakistan, The Egyptian Journal of Remote Sensing and Space Sciences, https://doi.org/10.1016/j.ejrs.2018.03.004

Table 1
Landslide inducing factors classes weights in the study area.

Factor	Classes (degree)	Number of Pixel in Class	Number of Pixel in Class % (a)	Number of Landslide Pixel in Class	Number of Landslide Pixel in Class % (b)	Frequency Ratio (FR) (b/a)
Slope	<10	234908	8.42	4467	3.08	0.37
	10–20	299519	10.73	10374	7.16	0.67
	20–30	383525	13.75	18153	12.52	0.91
	30–40	461865	16.55	26160	18.05	1.09
	40–50	483810	17.34	30756	21.22	1.22
	50–60	441623	15.83	28252	19.49	1.23
	60–70	328439	11.77	19147	13.21	1.12
	>70	156566	5.61	7640	5.27	0.94
Aspect						
	North	355314	12.73	11139	7.68	0.60
	Northeast	299312	10.73	8407	5.80	0.54
	East	316538	11.34	22457	15.49	1.37
	Southeast	317753	11.39	22761	15.70	1.38
	South	335037	12.01	17171	11.85	0.99
	Southwest	368225	13.20	17518	12.09	0.92
	West	414583	14.86	26221	18.09	1.22
	Northwest	383346	13.74	19273	13.30	0.96
Geology						
	Amphibolites	561	0.02	23	0.02	0.79
	Diorites and granodiorites	7667	0.28	350	0.24	0.88
	Ultramafics	337	0.01	47	0.03	2.67
	Gneiss	13337	0.48	799	0.55	1.15
	Limestone	141	0.01	7	0.01	0.96
	Marble	10	0.00	0	0.00	0
	Conglomerate	178	0.01	7	0.01	0.76
	Quaternary deposits	2278	0.08	206	0.14	1.73
	Volcanics	10929	0.39	576	0.40	1.01
	Terigeneous formation	3987	0.14	391	0.27	1.89
	Undifferentiated metasediments	204	0.01	0	0.00	0
Distance to stream						
	<20	23029	0.83	1075	0.74	0.90
	20–40	22742	0.82	1164	0.80	0.99
	40–60	22355	0.80	1317	0.91	1.13
	60–80	22232	0.80	1571	1.08	1.36
	80–100	21874	0.78	1794	1.24	1.58
	>100	2677951	95.98	138028	95.23	0.99
Distance to fault						
	<50	30222	1.08	2058	1.42	1.31
	51–100	30035	1.08	2083	1.44	1.33
	100–150	30043	1.08	2078	1.43	1.33
	150–200	30021	1.08	2117	1.46	1.36
	200–250	29960	1.07	2134	1.47	1.37
	>250	2636696	94.61	134479	92.78	0.98
Distance to road						
	<100	55733	2.000	11171	7.71	3.85
	100–200	50590	1.815	9870	6.81	3.75
	200–300	46503	1.669	9129	6.30	3.77
	300–400	42149	1.512	8218	5.67	3.75
	400–500	39722	1.425	7284	5.03	3.53
	>500	2552280	91.579	99277	68.49	0.75
Landcover						
	Water Body	21407	0.77	542	0.37	0.49
	Forest and shrub land	452452	16.23	21973	15.16	0.93
	Barren Land	656714	23.56	96405	66.51	2.82
	Alpine pasture and spare grass	434876	15.60	17820	12.29	0.79
	Irrigated agricultural land	116871	4.19	7416	5.12	1.22
	Permanent snow	1002486	35.96	219	0.15	0.00
	Glacier	102823	3.69	574	0.40	0.11

Please cite this article as: H. Khan, M. Shafique, M. A. Khan et al., Landslide susceptibility assessment using Frequency Ratio, a case study of northern Pakistan, The Egyptian Journal of Remote Sensing and Space Sciences, https://doi.org/10.1016/j.ejrs.2018.03.004

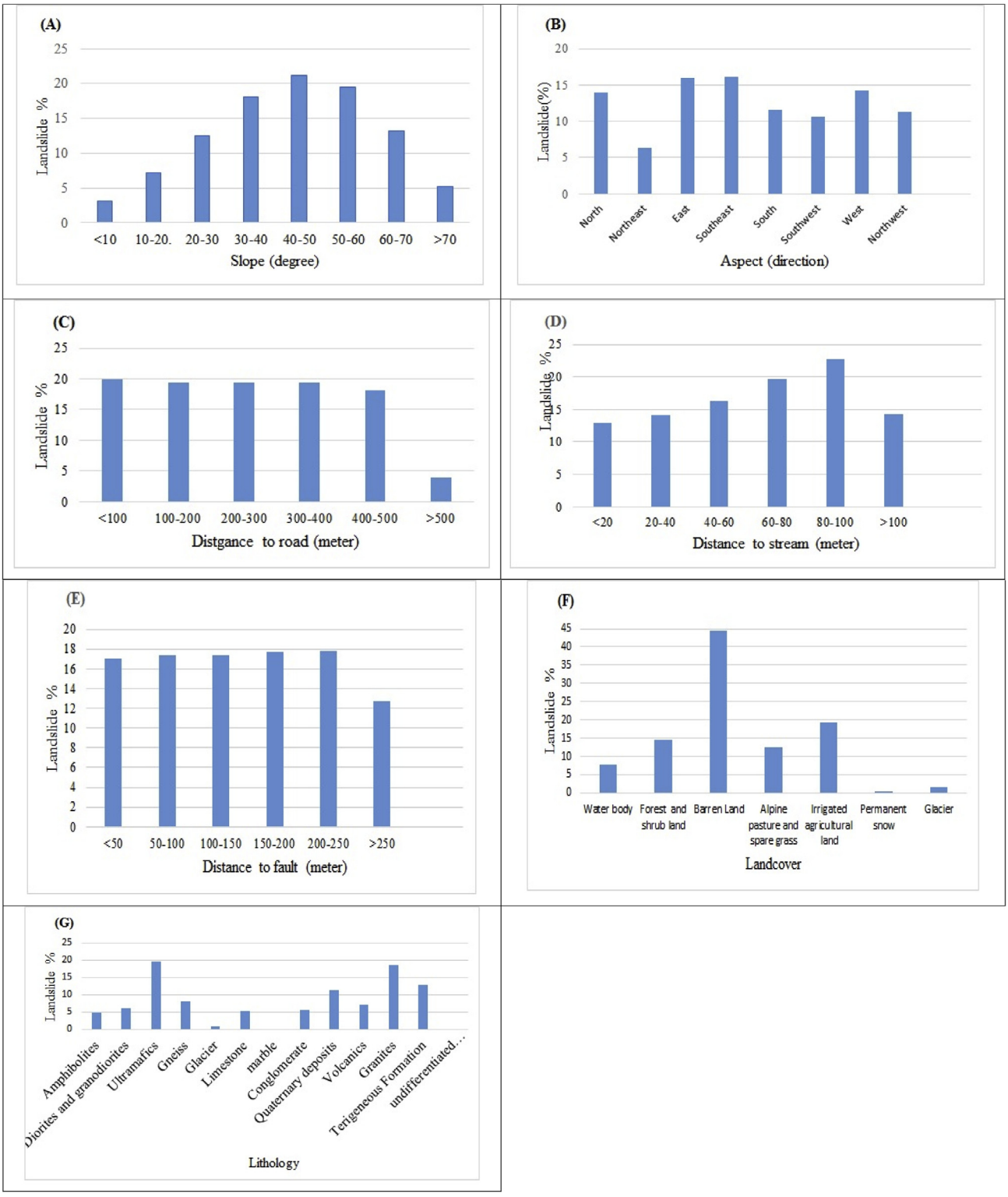

Fig. 7. Relationship of landslides occurrences with the causative factors. (a) terrain slope (b) terrain aspect, (c) distance to road (d) distance to stream (e) distance to fault, (f) landcover (g) geology.

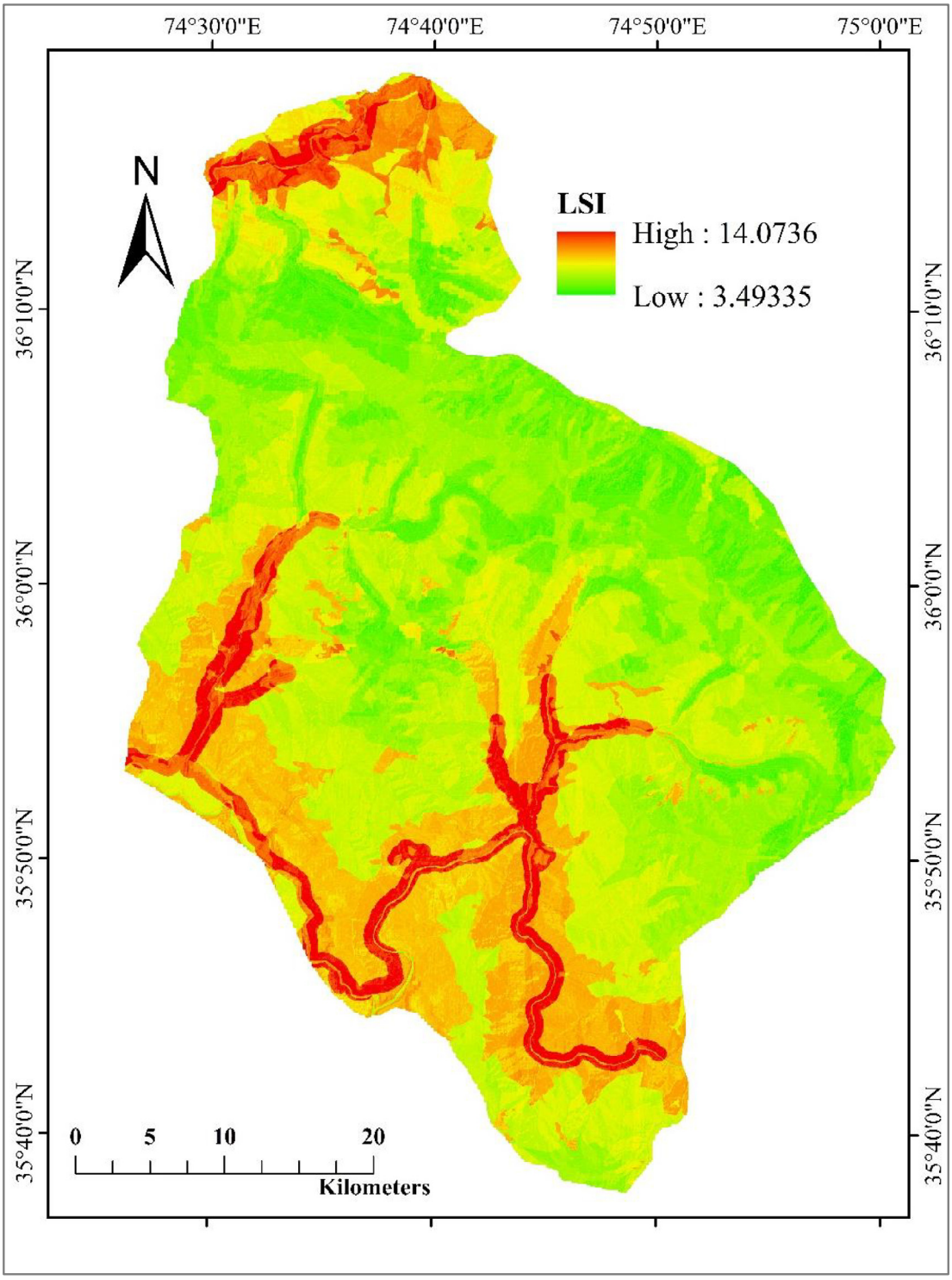

Fig. 8. Landslide susceptibility Index map of the study area.

very high susceptibility classes to develop a landslide susceptibility map for the study area (Fig. 9). The results indicate that 46.75% area falls in moderate class followed by low susceptibility class 35.94% while 13.41% area is recognized as high class and very highly susceptibility class is 3.90%.

Success rate curve is shown in the Fig. 10 which was used to validate the developed landslide susceptibility map (Fig. 9). The success rate curve is generated from the LSI map, shown in Fig. 8. All the index values of each pixel in the LSI map were then calculated. These values were reclassified into 100 classes with the 1% cumulative intervals. The classified map, was then crossed with the landslide inventory map. The validation results shown that 70% pixels are correctly classified as landslide pixels.

Please cite this article as: H. Khan, M. Shafique, M. A. Khan et al., Landslide susceptibility assessment using Frequency Ratio, a case study of northern Pakistan, The Egyptian Journal of Remote Sensing and Space Sciences, https://doi.org/10.1016/j.ejrs.2018.03.004

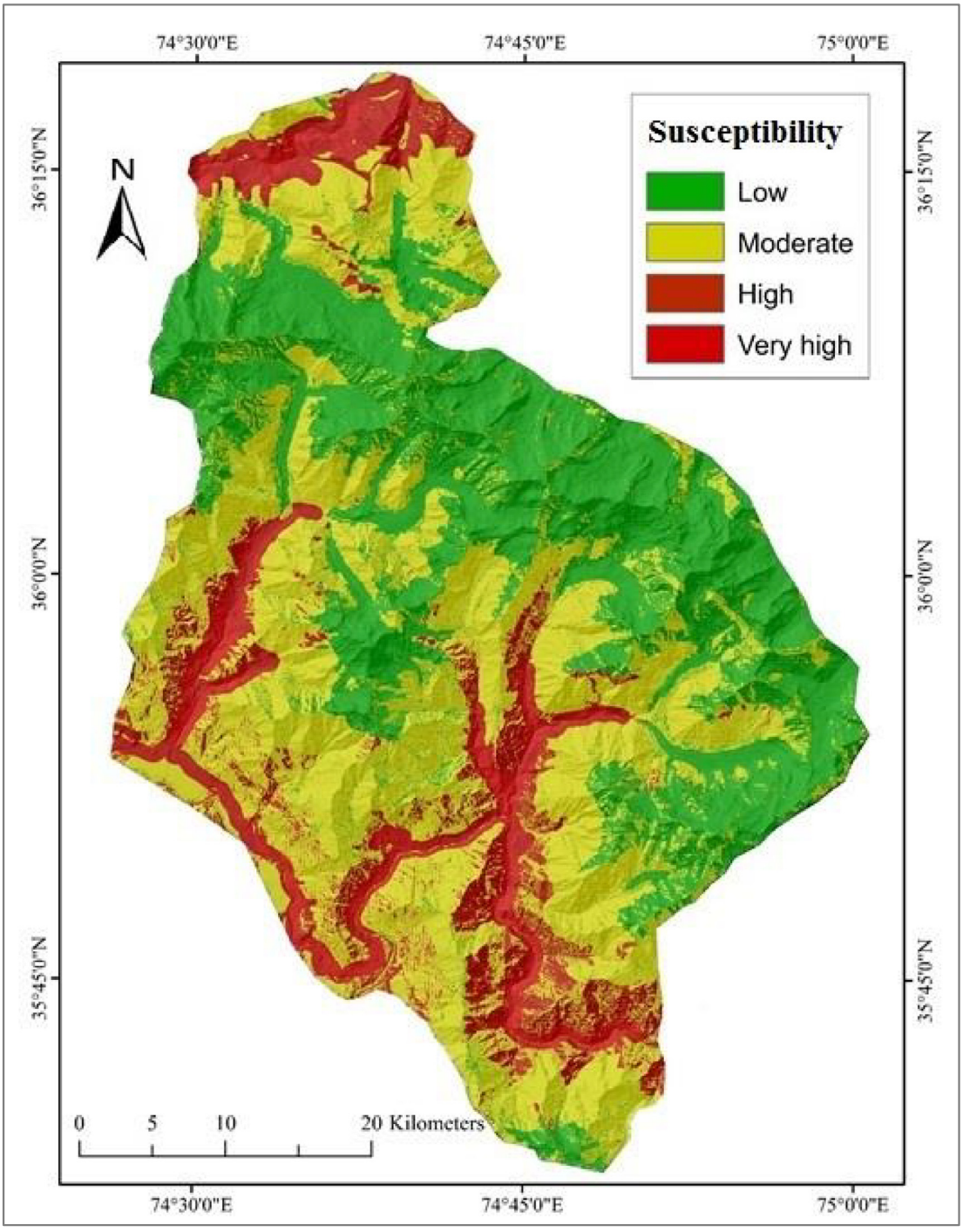

Fig. 9. Landslide susceptibility map of the study area.

5. Conclusion

In this study, remote sensing and GIS are effectively used to develop a landslide inventory, analysis their spatial distribution and develop a landslide susceptibility map. Based on the visual interpretation of the SPOT-5 image, landslide inventory is developed which is subsequently verified in the field.. The comparison of the landslide inventory with the landslide causative factors, showed that the roads and slope gradient are the most influential factors, controlling the spatial distribution of landslides in the area. The fractured and jointed lithology also significantly control on the spatial distribution of landslides. The barren area and irrigated agricultural land is also prone to slope failures in the area. The landslide intensity also increases as approaching to the roads and streams. The derived relationship between the landslide inventory and causative factors are used in the Frequency ratio technique to develop a landslide susceptibility map. The derived landslide susceptibility map, shows that 17.31% of the study area is identified as high to very high susceptible to landslides. The developed landslide susceptibility map can be utilized by the concern agencies to formulate and implement landslide mitigation measures.

Please cite this article as: H. Khan, M. Shafique, M. A. Khan et al., Landslide susceptibility assessment using Frequency Ratio, a case study of northern Pakistan, The Egyptian Journal of Remote Sensing and Space Sciences, https://doi.org/10.1016/j.ejrs.2018.03.004

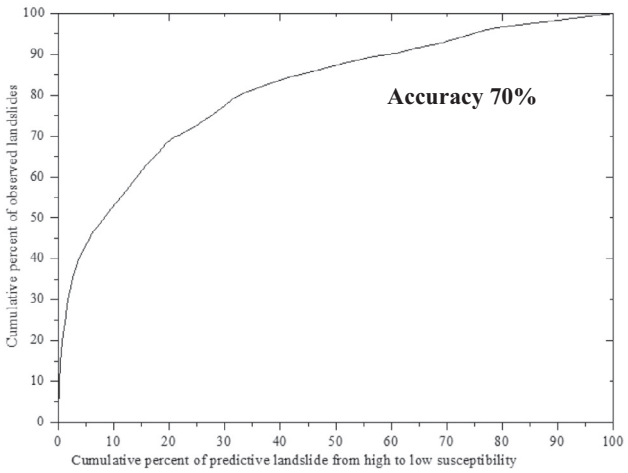

Fig. 10. Cumulative percentage of study area classified as susceptible (x-axis) in cumulative percent of landslide occurrence (y-axis).

Conflict of interest

None.

Acknowledgement

The authors would like to acknowledge the Karakorum International University, Gilgit-Pakistan and the Pakistan Science Foundation (grant number PSF/NSFC/Earth-KP-UoP (11)) for the financial support of the study.

References

Akgun, A., Dag, S., Bulut, F., 2007. Landslide susceptibility mapping for a landslide-prone area (Findikli, NE of Turkey) by likelihood-frequency ratio and weighted linear combination models. Eng. Geol. 54, 1127–1143.

Basharat, M., Rohn, J., Baig, M.S., Khan, M.R., 2014. Spatial distribution analysis of mass movements triggered by the 2005 Kashmir earthquake in the Northeast Himalayas of Pakistan. Geom 206, 203–214.

Bettinelli, P., Avouac, J.-P., Flouzat, M., Jouanne, F., Bollinger, L., PascalWillis and G. R. Chitrakar,, 2006. Plate motion of India and interseismic strain in the Nepal Himalaya from GPS and DORIS measurements. J. Geod. 80 (8–11), 567–589.

Bonham-Carter, G.F., 1994. Geographic Information Systems for Geoscientists. PERGAMON PRESS, Modeling with GIS, OXFORD.

Burrough, P.A., McDonell, R.A., 1998. Principles of Geographical Information Systems. Oxford University Press, New York.

Butler, R.W.H., Prior, D.J., 1988. Tectonic controls on the uplift of the Nanga Parbat Massif, Pakistan Himalayas. Nature 333 (6170), 247–250.

Chauhan, S., Sharma, M., Arora, M.K., 2010. Landslide susceptibility zonation of the Chamoli region, Garhwal Himalayas, using logistic regression model. Landslides 7 (4), 411–423.

Chen, W., Chai, H., Sun, X., Wang, Q., Ding, X., Hong, H., 2016a. A GIS-based comparative study of frequency ratio, statistical index and weights-of-evidence models in landslide susceptibility mapping. Arab. J. Geosci. 9 (3), 204.

Chen, W., Wang, J., Xie, X., Hong, H., Van Trung, N., Bui, D.T., Wang, G., Li, X., 2016b. Spatial prediction of landslide susceptibility using integrated frequency ratio with entropy and support vector machines by different kernel functions. Environ. Earth Sci. 75 (20), 1344.

Chen, X.L., Ran, H.L., Yang, W.T., 2012. Evaluation of factors controlling large earthquake-induced landslides by the Wenchuan earthquake. Nat. Hazards Earth Syst. Sci. 12 (12), 3645–3657.

Dahal, R.K., Hasegawa, S., Nonomura, A., Yamanaka, M., Dhakal, S., Paudyal, P., 2008. Predictive modelling of rainfall-induced landslide hazard in the Lesser Himalaya of Nepal based on weights-of-evidence. Geomorphology 102 (3–4), 496–510.

Derbyshire, E., Moniques, F., Owen, L.A., 2001. Geomorphological hazards along the Karakoram Highway: Khunjerab Pass to the Gilgit River, Northern Pakistan. Erdkunde 55, 49–71.

Devkota, K.C., Regmi, A.D., Pourghasemi, H.R., Yoshida, K., Pradhan, B., Ryu, I.C., Dhital, M.R., Althuwaynee, O.F., 2013. Landslide susceptibility mapping using certainty factor, index of entropy and logistic regression models in GIS and their comparison at Mugling-Narayanghat road section in Nepal Himalaya. Nat. Hazards 65 (1), 135–165.

Ding, Q., Chen, W., Hong, H., 2017. Application of frequency ratio, weights of evidence and evidential belief function models in landslide susceptibility mapping. Geocarto International 32 (6), 619–639.

Erener, A., Mutlu, A., Sebnem Düzgün, H., 2016. A comparative study for landslide susceptibility mapping using GIS-based multi-criteria decision analysis (MCDA), logistic regression (LR) and association rule mining (ARM). Eng. Geol. 203, 45–55.

ESRI. (2017). "Arc Hydro Overview." Retrieved 15 September 2017, from http://resources.arcgis.com/en/communities/hydro/01vn0000000s000000.htm.

Faraji Sabokbar, H., Shadman Roodposhti, M., Tazik, E., 2014. Landslide susceptibility mapping using geographically-weighted principal component analysis. Geomorphology 226, 15–24.

García-Rodríguez, M.J., Malpica, J.A., Benito, B., Díaz, M., 2008. Susceptibility assessment of earthquake-triggered landslides in El Salvador using logistic regression. Geomorphology 95 (3), 172–191.

Gorum, T., Fan, X., van Westen, C., Huang, R., Xu, Q., Tang, C., Wang, G., 2011. Distribution pattern of earthquake-induced landslides triggered by the 12 May 2008 Wenchuan earthquake. Geomorphology 133 (3–4), 152–167.

Harp, E.L., Keefer, D.K., Sato, H.P., Yagi, H., 2011. Landslide inventories: The essential part of seismic landslide hazard analyses. Eng. Geol. 122 (1–2), 9–21.

Hewitt, K., 1998. Catastrophic landslides and their effects on the Upper Indus streams, Karakoram Himalaya, northern Pakistan. Geomorphology 26 (1–3), 47–80.

Hung, L.Q., Van, N.T.H., Duc, D.M., Ha, L.T.C., Van Son, P., Khanh, N.H., Binh, L.T., 2015. Landslide susceptibility mapping by combining the analytical hierarchy process and weighted linear combination methods: a case study in the upper Lo River catchment (Vietnam). Landslides, 1–17.

Ilia, I., Tsangaratos, P., 2016. Applying weight of evidence method and sensitivity analysis to produce a landslide susceptibility map. Landslides 13 (2), 379–397.

Kamp, U., Growley, B.J., Khattak, G.A., Owen, L.A., 2008. GIS-based landslide susceptibility mapping for the 2005 Kashmir earthquake region. Geomorphology 101 (4), 631–642.

Kayastha, P., Dhital, M.R., De Smedt, F., 2013. Application of the analytical hierarchy process (AHP) for landslide susceptibility mapping: a case study from the Tinau watershed, west Nepal. Comput. Geosci. 52, 398–408.

Lee, S., Talib, J.A., 2005. Probabilistic landslide susceptibility and factor effect analysis. Environ. Geol. 47 (7), 982–990.

Lin, A., Guo, J., 2008. Co-seismic surface ruptures produced by the 2005 Pakistan M w7.6 earthquake in the Muzaffarabad area, revealed by QuickBird imagery data. Int. J. Remote Sens. 29 (1), 235–246.

Madin, I.P., Lawrence, R.D., Ur-Rehman, S., 1989. The northwestern Nanga Parbat–Haramosh Massif; Evidence for crustal uplift at the northwestern corner of the Indian Craton. Tectonics of the western Himalayas. In: Malinconico, J.L.L., Lillie, R.J. (Eds.), Geological Society of America.

Mansouri, D., Reza, M., 2014. Landslide susceptibility zonation using analytical hierarchy process and GIS for the Bojnurd region, northeast of Iran. Landslides 11 (6), 1079–1091.

Misch, P., 1949. Metasomatic granitization of batholithic dimensions. Am. J. Sci. 247 (4), 209–245.

Mondal, S., Maiti, R., 2013. Integrating the analytical hierarchy process (AHP) and the frequency ratio (FR) model in landslide susceptibility mapping of Shiv-khola watershed. Int. J. of Dis. Risk Sci. 4 (4), 200–212.

Nefeslioglu, H.A., Gokceoglu, C., Sonmez, H., 2008. An assessment on the use of logistic regression and artificial neural networks with different sampling strategies for the preparation of landslide susceptibility maps. Eng. Geol. 97 (3–4), 171–191.

Peduzzi, P., 2010. Landslides and vegetation cover in the 2005 North Pakistan earthquake: a GIS and statistical quantitative approach. Nat. Hazards Earth Syst. Sci. 10 (4), 623–640.

Petterson, M.G., Windley, B.F., 1985. RbSr dating of the Kohistan arc-batholith in the Trans-Himalaya of north Pakistan, and tectonic implications. Earth Planet. Sci. Lett. 74 (1), 45–57.

Pudsey, C.J., Coward, M.P., Luff, I.W., Shackleton, R.M., Windley, B.F., Jan, M.Q., 2011. Collision zone between the Kohistan arc and the Asian plate in NW Pakistan. Trans. R. Soc. Edinburgh: Earth Sci. 76 (4), 463–479.

Reis, S., Yalcin, A., Atasoy, M., Nisanci, R., Bayrak, T., Erduran, M., Sancar, C., Ekercin, S., 2012. Remote sensing and GIS-based landslide susceptibility mapping using frequency ratio and analytical hierarchy methods in Rize province (NE Turkey). Environ. Earth Sci. 66 (7), 2063–2073.

Rostami, Z.A., Al-modaresi, S.A., Fathizad, H., Faramarzi, M., 2016. Landslide susceptibility mapping by using fuzzy logic: a case study of Cham-gardalan catchment, Ilam, Iran. Arab. J. Geosci. 9 (17), 685.

Saaty, T.L., 1980. The Analytic Hierarchy Process: Planning, Priority Setting, Resources Allocation. McGraw-Hill, New York, NY.

Sayab, M., Khan, M.A., 2010. Temporal evolution of surface rupture deduced from coseismic multi-mode secondary fractures: Insights from the October 8, 2005 (Mw 7.6) Kashmir earthquake, NW Himalaya. Tectonophysics 493 (1–2), 58–73.

M.P. Searle, M.A. Khan, 1996. Geological map of northern Pakistan and adjacent areas of northern Ladakh and western Tibet.

Shafique, M., van der Meijde, M., Khan, M.A., 2016. A review of the 2005 Kashmir earthquake-induced landslides; from a remote sensing prospective. J. Asian Earth Sci. 118, 68–80.

Please cite this article as: H. Khan, M. Shafique, M. A. Khan et al., Landslide susceptibility assessment using Frequency Ratio, a case study of northern Pakistan, The Egyptian Journal of Remote Sensing and Space Sciences, https://doi.org/10.1016/j.ejrs.2018.03.004

Shahabi, H., Khezri, S., Ahmad, B.B., Hashim, M., 2014. Landslide susceptibility mapping at central Zab basin, Iran: a comparison between analytical hierarchy process, frequency ratio and logistic regression models. CATENA 115, 55–70.

Tien Bui, D., Tuan, T.A., Klempe, H., Pradhan, B., Revhaug, I., 2016. Spatial prediction models for shallow landslide hazards: a comparative assessment of the efficacy of support vector machines, artificial neural networks, kernel logistic regression, and logistic model tree. Landslides 13 (2), 361–378.

Treloar, P.J., Coward, M.P., 1991. Indian Plate motion and shape: constraints on the geometry of the Himalayan orogen. Tectonophysics 191 (3), 189–198.

Umar, Z., Pradhan, B., Ahmad, A., Jebur, M.N., Tehrany, M.S., 2014. Earthquake induced landslide susceptibility mapping using an integrated ensemble frequency ratio and logistic regression models in West Sumatera Province, Indonesia. CATENA 118, 124–135.

Wadia, D.N., 1961. The Geology of India. MacMillan, London.

Wang, Q., Li, W., 2017. A GIS-based comparative evaluation of analytical hierarchy process and frequency ratio models for landslide susceptibility mapping. Phys. Geogr. 38 (4), 318–337.

J.K. Weissel, C.P. Stark, 2001. Landslides triggered by the 1999 Mw7.6 Chi Chi earthquake in Taiwan and their relationship to topography. Geoscience and Remote Sensing Symposium, 2001. IGARSS '01. IEEE 2001 International.

Wu, Y., Li, W., Wang, Q., Liu, Q., Yang, D., Xing, M., Pei, Y., Yan, S., 2016. Landslide susceptibility assessment using frequency ratio, statistical index and certainty factor models for the Gangu County, China. Arab. J. Geosci. 9 (2), 1–16.

Yalcin, A., 2008. GIS-based landslide susceptibility mapping using analytical hierarchy process and bivariate statistics in Ardesen (Turkey): Comparisons of results and confirmations. CATENA 72 (1), 1–12.

Yalcin, A., Reis, S., Aydinoglu, A.C., Yomralioglu, T., 2011. A GIS-based comparative study of frequency ratio, analytical hierarchy process, bivariate statistics and logistics regression methods for landslide susceptibility mapping in Trabzon, NE Turkey. CATENA 85 (3), 274–287.

Yilmaz, I., 2009. Landslide susceptibility mapping using frequency ratio, logistic regression, artificial neural networks and their comparison: A case study from Kat landslides (Tokat—Turkey). Comput. Geosci. 35 (6), 1125–1138.

Please cite this article as: H. Khan, M. Shafique, M. A. Khan et al., Landslide susceptibility assessment using Frequency Ratio, a case study of northern Pakistan, The Egyptian Journal of Remote Sensing and Space Sciences, https://doi.org/10.1016/j.ejrs.2018.03.004